Supporting Information

Hydrated Manganese (II) Phosphate ($Mn_3(PO_4)_2$-$3H_2O$) as a Water Oxidation Catalyst

Kyoungsuk Jin[†,‡,⊥], Jimin Park[†,‡,⊥], Joohee Lee[†,‡], Ki Dong Yang[†,‡], Gajendra Kumar Pradhan[†,‡], Uk Sim[†,‡], Donghyuk Jeong[†,‡], Hae Lin Jang[†,‡], Sangbaek Park[†,‡], Donghun Kim[#], Nark-Eon Sung[§], Sun Hee Kim[#], Seungwu Han[†,‡], Ki Tae Nam[†,‡*]

[†]Department of Materials Science and Engineering, Seoul National University, Seoul 151-744, Korea

[‡]Research Institute of Advanced Materials (RIAM), Seoul National University, Seoul 151-744, Korea

[#]Division of Materials Science, Korea Basic Science Institute, Daejeon, 305-333, Korea

[§]Pohang Accelerator Laboratory, POSTECH, Pohang, 790-784, South Korea

[⊥] These authors contributed equally to this work.

*To whom correspondence should be addressed.

E-mail: nkitae@snu.ac.kr

A. Materials and Methods

A1. Materials

$MnCl_2$-**4**H_2O (99 %), HEPES (2-4-(2-hydroxyethyl)-1-piperazinyl)Ethane-sulfonic acid) (99 %), KH_2PO_4 (99 %), Nafion 117 solution (5 wt % in aliphatic alcohols and water), Na_2HPO_4-**7**H_2O (ACS reagent, 98.0-102.0 %), and NaH_2PO_4-**2**H_2O (99.0 %) were purchased from Sigma Aldrich and used as received without further purification. Fluorine doped Tin-Oxide coated glass (FTO, TEC-8) which has 15 Ω sq^{-1} surface resistivity was obtained as pre-cut by 1.0 cm × 1.5 cm glass pieces from Pilington Company.

A2. Synthesis of $Mn_3(PO_4)_2$-**3**H_2O

Manganese (II) phosphate hydrate was synthesized by adding 40 ml of 1.0 mM KH_2PO_4 in HEPES (1.85 mM, pH 7.4) to 40 mL of 1.0 mM $MnCl_2$-**4**H_2O solution at 37°C. The mixed solution slowly became turbid, indicating the formation of manganese (II) phosphate hydrate. After 3 h, the precipitate was centrifuged and washed three times with deionized (DI) water. Collected particles were then lyophilized before characterization.

A3. Powder X-ray diffraction

Powder X-ray diffraction (XRD) was carried out on a D-8 Advance X-ray diffractometer with Cu Kα radiation (λ=1.54056Å). For the measurement, precipitated $Mn_3(PO_4)_2$-**3**H_2O powder was collected and lyophilized at least 2 days. The lyophilized powder was loaded on Si holder, retrofitted in X-ray diffractometer. XRD patterns were recorded in a range of 5 ~ 100° with a step of 0.02° and a velocity of 0.02°/16 s. Obtained XRD patterns were compared with previously reported JDPDS cards.

A4. Scanning electron microscopy (SEM) Analysis

The morphology of synthesized $Mn_3(PO_4)_2$-**3**H_2O was characterized with a high resolution scanning electron microscope (Supra 55VP, Carl Zeiss, Germany). The samples were investigated right after the electrochemical measurements or formation of $Mn_3(PO_4)_2$-**3**H_2O flower like plates on FTO glasses. The samples were rinsed gently with deionized water at least 3 times and dried with nitrogen gas. Pt coating was done by Pt Sputter Coater (BAL-TEC/SCD 005) because $Mn_3(PO_4)_2$-**3**H_2O particles were not conductive enough. Images were taken with an acceleration voltage of 2 kV, and EDX spectra with a 15 kV. Sample positions coincided with the illuminated area.

A5. Transmission electron microscopy (TEM) Analysis

TEM images and selected area electron diffraction (SAED) patterns were obtained using a high resolution transmission electron microscope (JEM-3000F, JEOL, Japan) with an acceleration voltage of 300 kV. The TEM samples were collected from FTO glass right after the catalyst formation or electrochemical measurement, and dispersed in ethanol by sonication about 1 min. About 10 μl of dispersed $Mn_3(PO_4)_2$-**3**H_2O were dropped on the TEM grid and dried in an oven.

A6. Elemental analysis

Inductively Coupled Plasma-Mass Spectrometer (ICP/MS, 720-ES, Varian) measurement was conducted to determine the exact chemical composition of $Mn_3(PO_4)_2$-**3**H_2O.

A7. Thermo Gravimetric analysis (TGA) analysis

Thermo Gravimetric analysis (TGA) was performed on the lyophilized $Mn_3(PO_4)_2$-$3H_2O$ powder described above. 2.177 mg of the samples were loaded to Thermo gravimetric analyzer(Q-5000 IR, TA instrument, USA) and its weight loss measured in a range of 25~500℃ with 5℃ min^{-1}.

A8. BET analysis

Brunauer-Emmett-Teller (BET) analysis was conducted on the lyophilized $Mn_3(PO_4)_2$-**3**H_2O powder. 0.5070 g of the sample was loaded to BET analyzer (Physisorption Analyzer, micromeritics, USA) under N_2 adsorption environment.

B. Structure analysis

B1. Crystal Structure analysis and Rietveld refinement

The crystal structure of switzerite was obtained from American Mineralogist Crystal Structure Database (AMCSD). The presumed crystal structure of the $Mn_3(PO_4)_2$-**3**H_2O was drawn with CrystalMaker (CrystalMaker Software) based on its atom coordination information. The maximum bond length between manganese atom and oxygen atom was set to 2.5 Å. Local structure around the P(1) site was visualized by defining the spherical cluster around the P(1) site at the radius of 4.5 Å. The final structure of $Mn_3(PO_4)_2$-**3**H_2O was refined by Rietveld refinement using TOPAS Academic.[s1]

C. Electrochemical measurements

C1. Electrochemical Methods

All electrochemical experiments were conducted under a three-electrode electrochemical cell system. A BASi Ag/AgCl/3M NaCl reference electrode and a Pt foil (2 cm × 2 cm × 0.1 mm, 99.997% purity, Alfa Aesar) were used as a reference electrode and a counter electrode, respectively. Electrochemical tests were carried out at ambient temperature (21 ± 1℃) using a potentiostat system (CHI 600D, CH Instruments). Electrode potential was converted to the NHE scale, using the following equation: E(NHE) = E(Ag/AgCl) + 0.197 V. Additionally, overpotential values were calculated by the difference between the iR corrected potential ($V = V_{applied} - iR$) and the thermodynamic point of water oxidation at a specified pH. The electrolyte was phosphate buffer with 500mM buffer strength under the pH 7. The electrolyte was degassed by bubbling with high-purity nitrogen (99.999 %) for at least 1 hour prior to the start of each experiment and stirred vigirously during the measurement to prevent the mass trasfort problem.

C2. Cyclic Voltammetry

The preparation procedure of the working electrodes containing our catalysts can be found as follows. Firstly, 5 mg of catalyst powder was dispersed in 1 ml of water mixed solvent with 100 μl of neutralized Nafion solution. Then the mixture was sonicated for at least 30 min to make homogeneous ink. Next, 50 μl of the catalyst solution was dropped onto the FTO substrate and spin-coating was performed at 3000 rpm for 30sec. Finally, prepared working electrode was dried at 80℃ oven before CV measurement. The working electrode was cycled at least 3 times with the potential stepped from 0.7 V to 1.5 V without pause at a scan rate of 10 mV sec^{-1} before all electrochemical data were recorded. Prior to every electrochemical experiment, the solution resistance was measured in the electrolysis bath. All the data were iR-compensated.

D. Computational Study

The first-principles density functional theory (DFT) calculations were performed with GGA+U functional using the Vienna *Ab*-initio simulation package (VASP) code. [s2, s3] Electron-ion interactions were approximated by the projected augmented wave (PAW) method.[s4] The effective *U* parameter of 4.0 eV was used for Mn d orbitals.[s5] The cutoff energy for plane-wave basis set was consistently chosen to be 800 eV, and the k-space was sampled by a 2 × 2 × 2 regular mesh. Atomic positions and lattice parameters were relaxed until the force and stress were reduced below 0.02 eV $Å^{-1}$ and 2 kbar. The atomic charges were estimated by the Bader analysis [s6] for prisine $Mn_3(PO_4)_2$-**3**H_2O, oxidized Mn phosphate, β-MnO_2, and reduced Mn oxide.

E. Supporting Tables

Oxide compound	System	Phosphate compound	System
MnO	Cubic ($Fm3m$)	**$Mn_2P_2O_7$**	Monoclinic($C2/m$)
Mn_2O_3	Orthorhombic ($P\ bca$)	**$Mn_3(PO_4)_2$**	Monoclinic($P2_1/a$)
MnOOH	Monoclinic ($B2_1/d$)	**MnP_4O_{11}**	Triclinic ($\bar{P}1$)
Mn_3O_4	Tetragonal ($I\ 4_1/amd$)	**$Mn_2P_4O_{12}$**	Monoclinic ($C2/c$)
MnO_2	Tetragonal ($P4_2/mnm$)	**$Mn_3(PO4)_2$**	Monoclinic ($C2_1/c$)
$MnFe_2O_4$	Tetragonal ($P4_2/nnm$)	**$Mn(PO_3)_3$**	Orthorhombic ($Pnaa$)
CoMnO	Cubic, Tetragonal ($I4_1/amd$)	**$Mn_3(PO_4)_2$ -3H_2O**	Triclinic (Our work)

Table S1

Crystal structures of manganese based oxide and phosphate compounds. It showed that almost all manganese oxide compounds display higher symmetry than manganese phosphate compounds. (All data were referred from JCPDS Card.)

Mn1	Mn2	Mn3	Mn4	Mn5	Mn6
2.210 Å	2.286 Å	2.163 Å	2.259 Å	2.214 Å	2.177 Å
2.145 Å	2.173 Å	2.286 Å	2.281 Å	2.208 Å	2.104 Å
2.119 Å	2.359 Å	2.262 Å	2.147 Å	2.316 Å	2.108 Å
2.317 Å	2.240 Å	2.218 Å	2.171 Å	2.120 Å	2.135 Å
2.139 Å	2.117 Å	2.264 Å	2.215 Å	2.121 Å	2.442 Å
2.468 Å	2.164 Å	2.175 Å	2.180 Å		

Table S2

Bond lengths between manganese and neighboring oxygen atoms in $Mn_3(PO_4)_2$-**3**H_2O. Average Mn-O bond distance is 2.215 Å

	Mn1	Mn2	Mn3	Mn4	Mn5
Edge Sharing	3.259 Å 3.398 Å	3.348 Å 3.208 Å	3.348 Å 3.295 Å	3.398 Å 3.337 Å	3.526 Å
Corner Sharing	3.664 Å	3.718 Å	3.664 Å	3.718 Å 3.609 Å	3.609 Å

Table S3

Mn-Mn distance in $Mn_3(PO_4)_2$-**3**H_2O. Distance values between edge-sharing manganese atoms and corner-sharing manganese atoms were obtained. Average Mn-Mn bond distance was 3.412 Å. Generally, corner sharing manganese atoms had larger Mn-Mn distances than edge sharing ones.

F. Supporting Figures

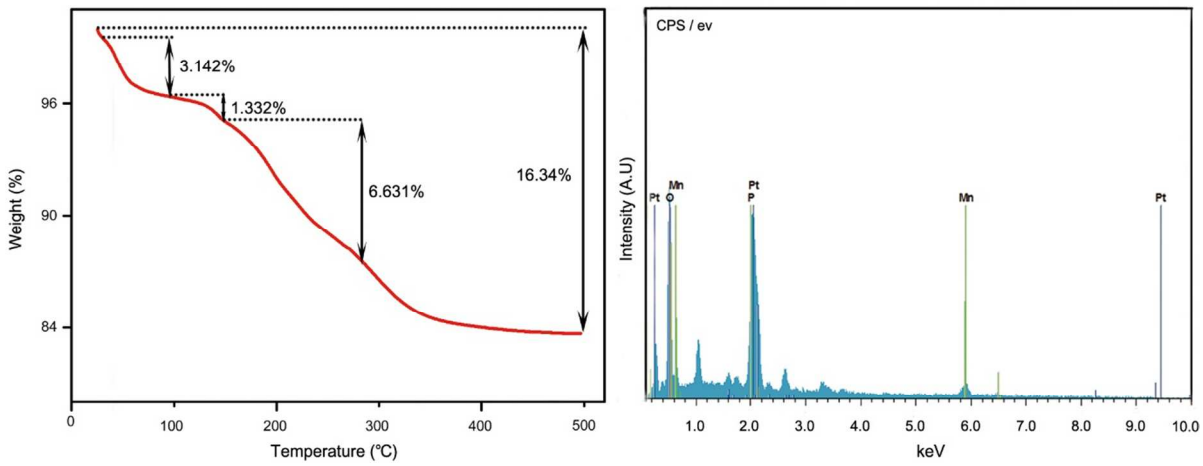

	Atomic weight	Solution concentration	Molar ratio
Mn	54.938	6.92	3
P	30.974	2.49	1,92

Figure S1

Thermogravimetric analysis (TGA) of $Mn_3(PO_4)_2$-$3H_2O$ from 25℃ to 500℃. The first drop of weight showed evaporation of H_2O molecules attached on the surface. Sequential weight drops of $Mn_3(PO_4)_2$-$\mathbf{3}H_2O$ indicated that H_2O molecules were intercalated in $Mn_3(PO_4)_2$-$\mathbf{3}H_2O$ structure. With the total weight loss (13.198 %) during TGA analysis, except that generated by surface water molecules, we could draw that three H_2O were embedded in manganese phosphate structure. And we also obtained from the ICP-MS result and EDS analysis that the ratio of manganese and phosphate was 3:2. Based on these results, we concluded that chemical formula of our catalyst was $Mn_3(PO_4)_2$-$\mathbf{3}H_2O$.

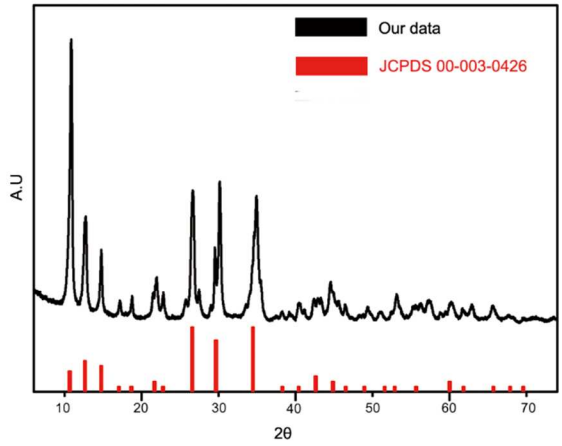

JCPDS 00-003-0426	Comments
Experimental Reference	The Dow Chemical Company, Midland, Michigan, USA. *Private Communication*
Chemical Formula	$Mn_3(PO_4)_2$-**3**H_2O
Empirical Formula	H6Mn3O11P2
Weight %	H1.48 Mn40.32 O43.05 P15.15
Atomic %	H27.27 Mn13.64 O50.00 P9.09
Physical Information	None
Crystal Information	None (Molecular weight = 408.8)
Structure Data	None (Centrosymmetric)

Figure S2

Comparison between XRD pattern of our $Mn_3(PO_4)_2$-**3**H_2O and previously reported JCPDS pattern of $Mn_3(PO_4)_2$-**3**H_2O. The JCPDS card data was significantly different from our data in terms of peak positions and peak intensity.

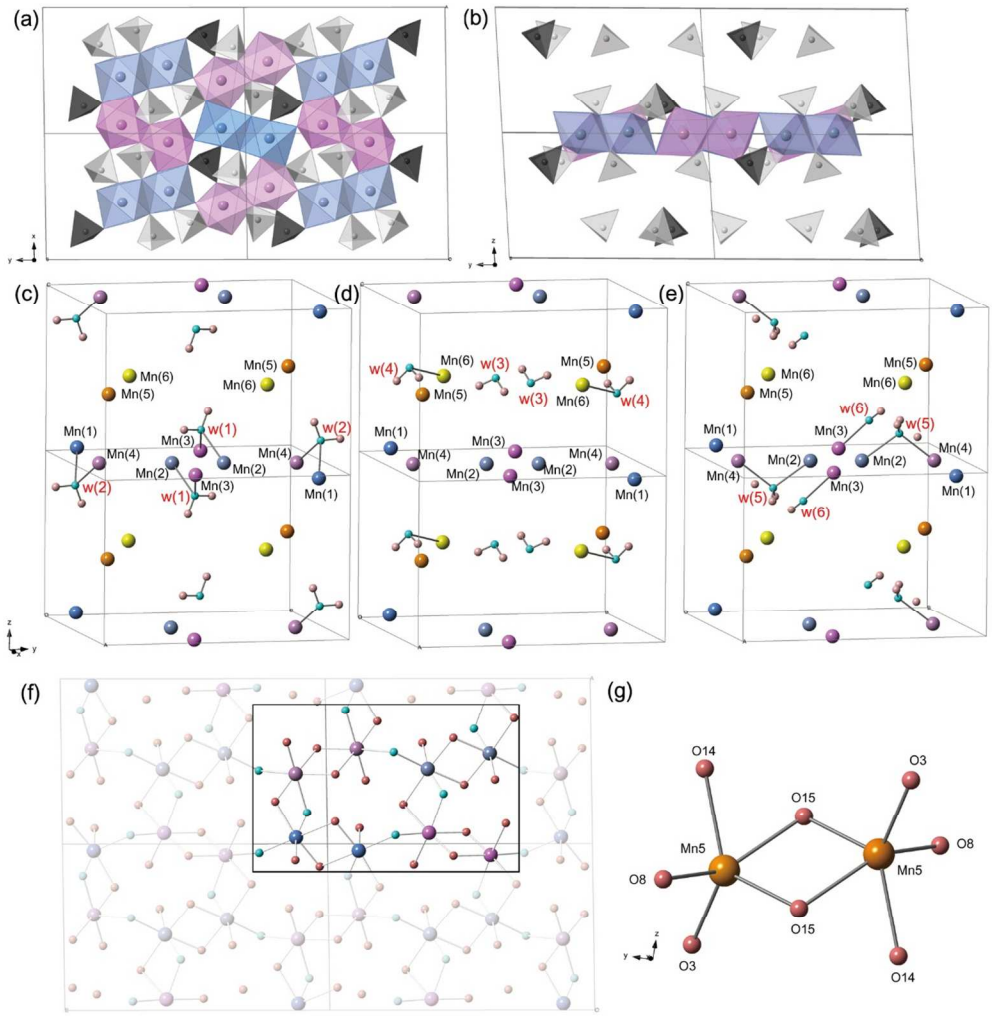

Figure S3

(a, b) Crystal structure of $[Mn_4O_{10}(H_2O)_2]_2$ sheet composed of Mn(1), Mn(2), Mn(3), and Mn(4). Mn(5) and Mn(6) were omitted for clarity. (c) Chemical environment around water (1) and water (2) molecules. Water (1) were ligated to both Mn(2) and Mn(3) atoms, and water (2) were ligated to Mn(1) and Mn(4) atoms. (d) Chemical environment around water (3) and water (4). In the case of water (3), no chemical bond existed around water (3), while water (4) were solely ligated to Mn(6) atom. (e) Chemical environment around water (5) and water (6). Water (5) were ligated together with Mn(2) and Mn(4) atoms. Water (6) were only ligated to Mn(3) atoms. (f) Chemical structure of $[Mn_4O_{10}(H_2O)_2]_2$ unit cell. (g) Chemical structure of Mn_2O_8 dimer involving two Mn(5) atoms.

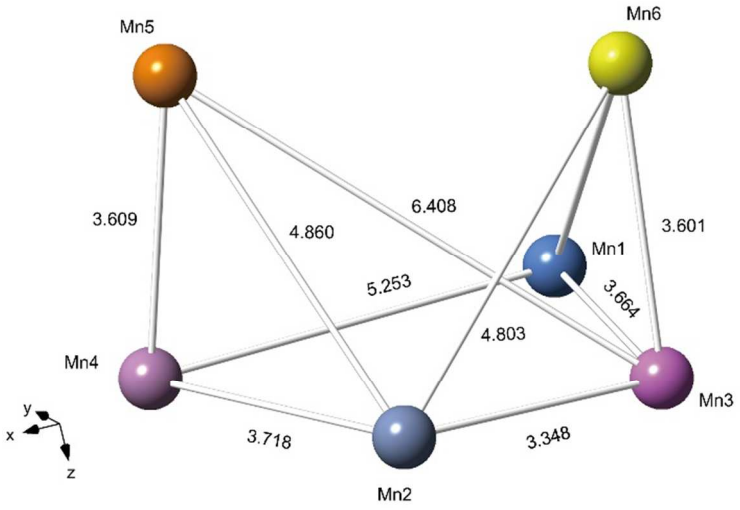

Figure S4

Distance between different manganese sites. Oxygen, hydrogen, and phosphate atoms were omitted for clarity from Figure 1e. All units were angstrom. The longest distance was 6.408 Å between Mn(3) and Mn(5) and the shortest was 3.348 Å between Mn(2) and Mn(3).

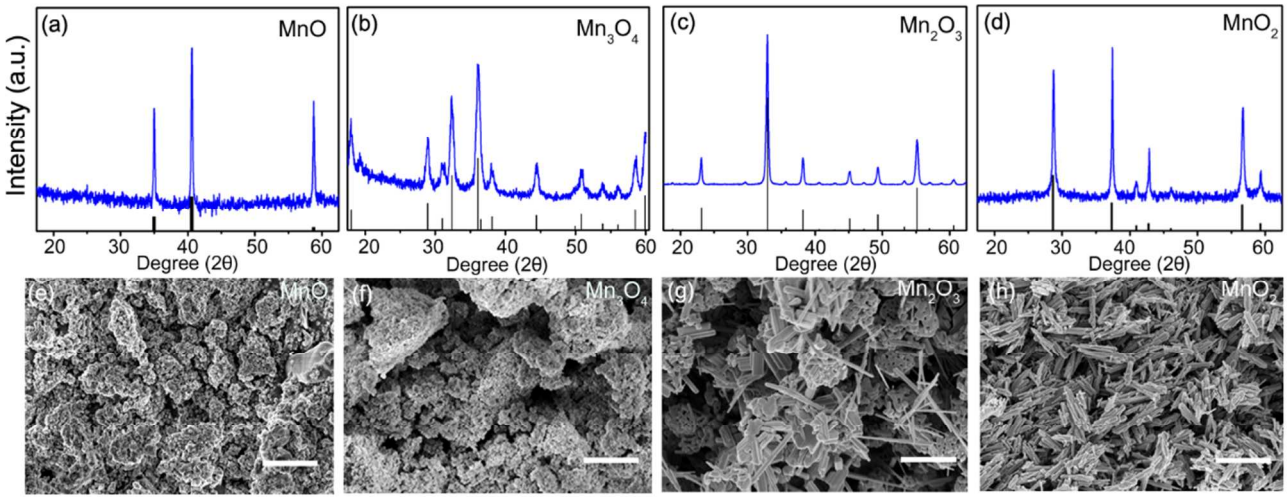

Figure S5

Characterization of synthesized MnO, Mn_3O_4, Mn_2O_3 and MnO_2 nanoparticles. (a-d) XRD patterns and (e-h) SEM images of MnO, Mn_3O_4, Mn_2O_3 and MnO_2 nanoparticles. (Scale bar : 1μm)

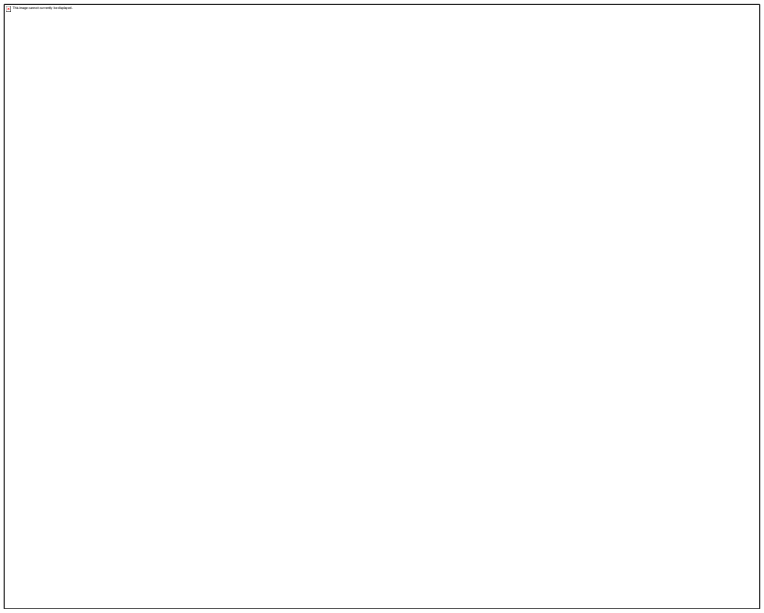

Figure S6

Cyclic voltammetry curves for five catalysts before polarization correction : $Mn_3(PO_4)_2$-**3**H_2O (red), nano MnO (pink), Mn_3O_4 (blue), Mn_2O_3 (dark yellow), and MnO_2 (black) Catalyst loaded working electrode were scanned at the rate of 10 mV sec^{-1} in 0.5 M phosphate buffer solution at applied potentials ranging from 0.7 V to 1.5 V.

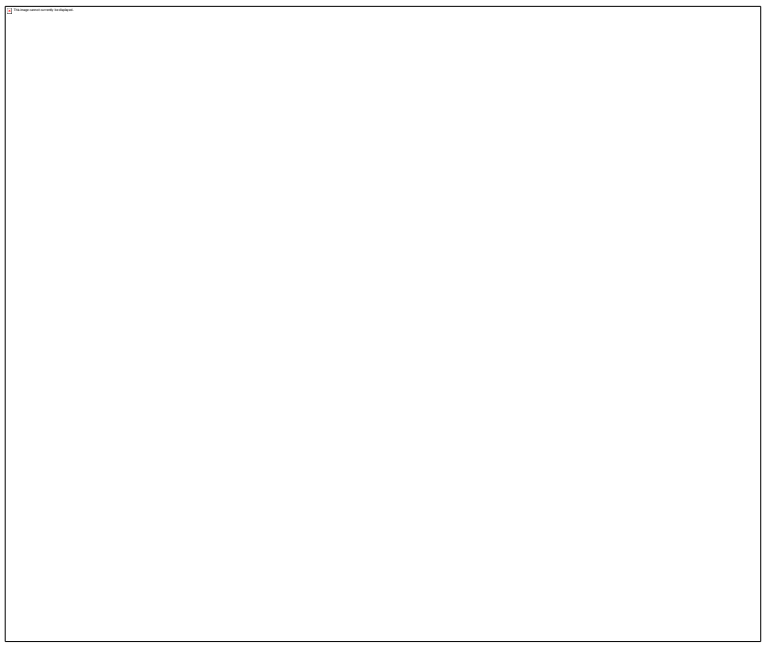

Figure S7

X-ray diffraction analysis of $Mn_3(PO_4)_2$-$3H_2O$ after bulk electrolysis at 1.0, and 1.5 V for 30 min. As shown in the figure, XRD analysis indicates that the phase remained after electrolysis, without the appearance of any other phases or any broadening of the peaks.

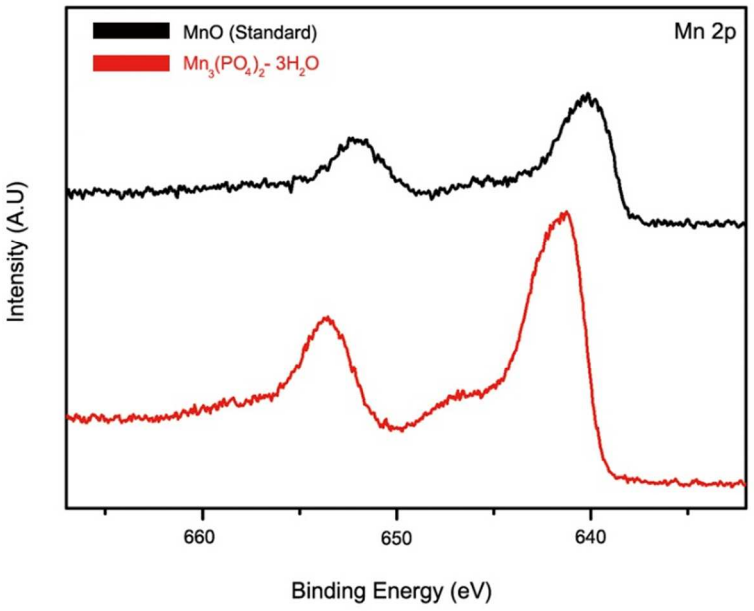

Figure S8

X-ray photo-electron spectroscopy of $Mn_3(PO_4)_2$-$3H_2O$ and MnO standard sample in the Mn 2p region. The spectra were calibrated to C-1s at 285.0 eV. As shown in the figure, $2p_{1/2}$ satellite structure displayed typical Mn^{2+} characteristic peaks in both samples, [s7] yet peak positions were shifted. To be specific, MnO have 640.2 eV , 652.4eV whereas $Mn_3(PO_4)_2$-$3H_2O$ have 641.25 eV, 653.75 eV peak positions, respectively. These results clearly revealed that Mn^{2+} atoms in $Mn_3(PO_4)_2$-$3H_2O$ have more nucleophilic character than those in MnO.

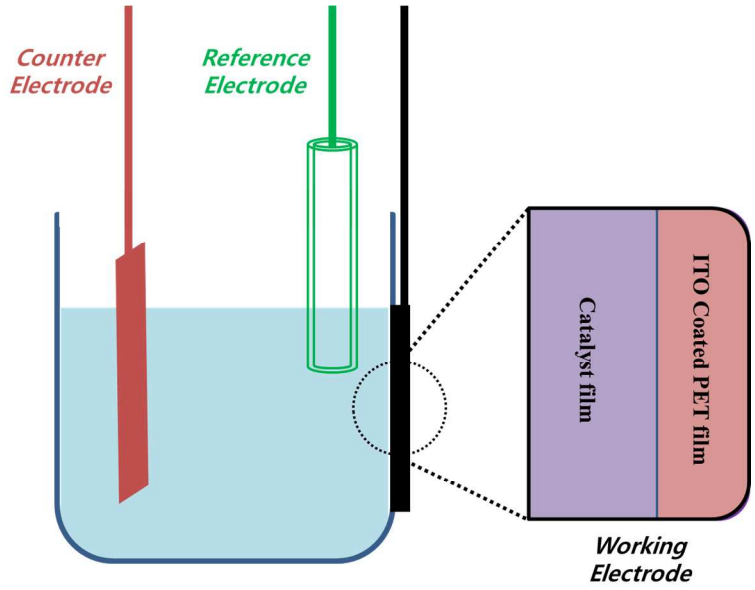

Figure S9

Scheme for designed electrochemical cell for *in-situ* XANES analysis. The electrochemical cell had a flat glass wall with a rectangular window (1.5 cm × 1.5 cm). A 3 cm × 3 cm piece of ITO-coated polyethylene terephthalate (ITO-PET, Kintec Company) was covered the outside of the window and ITO face was faced into the interior of the cell. The catalyst was deposited onto the ITO face and bulk-electrolysis was performed during the XAS measurement in this setup. We referenced similar approaches performed by Jaramillo group. [s8]

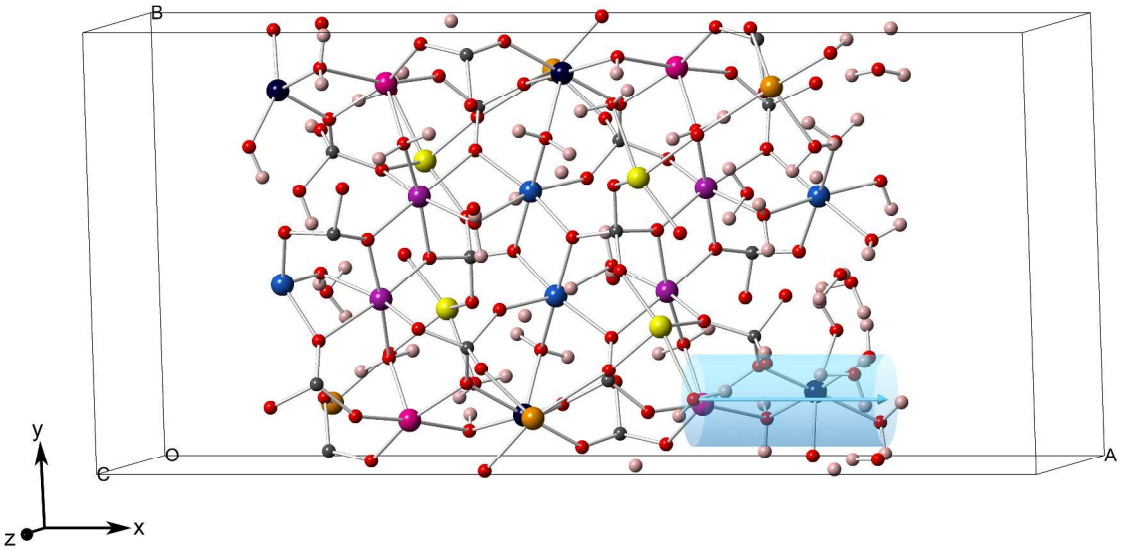

Figure S10

Surface structure of $Mn_3(PO_4)_2$-$3H_2O$. As indicated in the blue cylinder, the 5-fold Mn(6) at the subsurface are bonded to a water molecule, and there exists the channel where water molecules can access.

References

[s1] F. Izumi, R. Young, *by RA Young, The Rietveld Method, Oxford University Press, Oxford* **1993**, 236-253

[s2] G. Kresse, J. Hafner, *Phys. Rev. B* **1993**, *47*, 558-561.

[s3] G. Kresse, J. Furthmüller, *Phys. Rev. B* **1996**, *54*, 11169-11186.

[s4] G. Kresse, D. Joubert, *Phys. Rev. B* **1999**, *59*, 1758-1775.

[s5] L. Wang, T. Maxisch, G. Ceder, *Phys. Rev. B* **2006**, *73*, 195107.

[s6] W. Tang, E. Sanville, G. Henkelman, *J. Phys.: Condens. Matter* **2009**, *21*, 084204.

[s7] Gorlin, Y.; Jaramillo, T. F. *J. Am. Chem. Soc.* **2010**, 132, 13612.

[s8] Gorlin, Y.; Lassalle-Kaiser, B.; Benck, J. D.; Gul, S.; Webb, S. M.; Yachandra, V. K.; Yano, J.; Jaramillo, T. F. *J. Am. Chem. Soc.* **2013**, 135, 8525.